Original Research

Hybrid Donnan dialysis–electrodialysis for efficient ammonia recovery from anaerobic digester effluent

Zhinan Dai [a], Cong Chen [a], Yifan Li [a], Haoquan Zhang [a], Jingmei Yao [a], Mariana Rodrigues [b, c], Philipp Kuntke [b, c], Le Han [a, *]

[a] Key Laboratory of the Three Gorges Reservoir Region's Eco-Environment, Ministry of Education, College of Environment and Ecology, Chongqing University, Chongqing, 400045, PR China
[b] Wetsus, European Centre of Excellence for Sustainable Water Technology, Oostergoweg 9 8911MA Leeuwarden P.O. Box 1113, 8900 CC, Leeuwarden, the Netherlands
[c] Environmental Technology, Wageningen University, Bornse Weilanden 9 6708 WG Wageningen P.O. Box 17, 6700 AA, Wageningen, the Netherlands

A R T I C L E   I N F O

A B S T R A C T

Ammonia recovery from wastewater is crucial, yet technology of low carbon emission and high ammonia perm-selectivity against complex stream compositions is urgently needed. Herein, a membrane-based hybrid process of the Donnan dialysis–electrodialysis process (DD–ED) was proposed for sustainable and efficient ammonia recovery. In principle, DD removes the majority of ammonia in wastewater by exploring the concentration gradient of NH_4^+ and driven cation (Na^+) across the cation exchange membrane, given industrial sodium salt as a driving chemical. An additional ED stage driven by solar energy realizes a further removal of ammonia, recovery of driven cation, and replenishment of OH^- toward ammonia stripping. Our results demonstrated that the hybrid DD–ED process achieved ammonia removal efficiency >95%, driving cation (Na^+) recovery efficiency >87.1% for synthetic streams, and reduced the OH^- loss by up to 78% compared to a standalone DD case. Ammonia fluxes of 98.2 g_N m^{-2} d^{-1} with the real anaerobic digestion effluent were observed using only solar energy input at 3.8 kWh kg_N^{-1}. With verified mass transfer modeling, reasonably controlled operation, and beneficial recovery performance, the hybrid process can be a promising candidate for future nutrient recovery from wastewater in a rural, remote area.

1. Introduction

Nitrogen (N) is in an unsustainable open-loop state, considering the high cost of synthesizing N-based fertilizer and eliminating the N from wastewater (especially by the mainstream biological method) [1–3]. The recovery of ammonia, a representative reactive N from wastewater, is crucial [4,5]. Herein, ammonia as a general term is used to refer to both ammonium (ionic NH_4^+) and ammonia (volatile NH_3). Although many efforts like adsorption [6,7], struvite precipitation [8,9], and air stripping [10] have been put into ammonia recovery, these conventional recovery processes are suffering from high cost, low efficiency, and secondary pollution.

Many membrane-based ammonia recovery processes have been well-developed [11–13]. Taking the membrane stripping process as an example, the direct addition of alkali into the feed to increase the pH (toward converting ammonium to ammonia) could trigger the fouling/wetting issue for hydrophobic membrane coupon [14]. The inefficiency of alkali dosage due to the presence of impurities like multivalent cations (Ca^{2+}) and the dilution effect due to a large stream volume is also problematic, which in fact, applies to most stripping processes [15]. We argue that if ammonium has been selectively enriched out of the complex matrix in the feed, the remaining stripping step would be very effective with a precisely targeted dosage of alkali [16]. Recently, membrane-based electrochemical processes have drawn attention for their high efficiency, selectivity, and product purity in dealing with complex streams [17–19]. In such a scheme, migration of NH_4^+ across cation exchange membrane (CEM) from anode to cathode under current is effectively realized in an electrodialysis (ED) system, which is then converted into NH_3 for later stripping owing to the high pH of the

* Corresponding author.
  E-mail address: lehan@cqu.edu.cn (L. Han).

catholyte [11,20,21]. Nevertheless, two issues remain: (1) the electrochemical processes require non-negligible energy input, despite some recent efforts to reduce the energy consumption [18,22,23]; (2) protons (H^+) generated at the anode reduced the transfer efficacy or transport number of NH_4^+.

To this end, exploiting renewable energy sources, such as solar energy, definitely can be a more sustainable way for ammonia recovery, and that has already successfully supported several electrochemical pilot studies [24–26]. Meanwhile, exploring the concentration gradient-driven NH_4^+ diffusion instead of current-driven NH_4^+ migration, even only for a part-time, could save energy and reduce the H^+ generation accumulation (thus improving the transfer efficacy for NH_4^+). Ion-exchange membrane-based Donnan Dialysis (DD) process is reported to allow the expected NH_4^+ diffusion free of external energy consumption [23,27,28]. Noteworthy, such a DD-based ammonia recovery was at the cost of a limited NH_4^+ flux and a high chemical usage for driving the cation of Na^+, which is finally lost into the wastewater [28].

In this study, we proposed combining DD driven by waste salt (e.g., from a desalination process concentrate) with intermittent ED powered by solar energy for efficient and sustainable ammonia recovery from wastewater at low energy cost and low chemical consumption via recovering driving cation (Na^+). We hypothesize that without current, DD utilizes the concentration difference of NH_4^+ and Na^+ across the CEM to remove NH_4^+ without energy consumption and H^+ generated. At the end of the DD stage, the remaining ions (i.e., NH_4^+, Na^+) would migrate under current to further reduce NH_4^+ concentration in the anode or improve the overall NH_4^+ flux, recover Na^+ and replenish OH^- (favoring NH_3 stripping) in the cathode. Using brine to drive salt and solar energy would add to the process sustainability for ammonia recovery. The predictive modeling for this novel hybrid process was established to guide its smart operation, and the recovery performance with synthetic wastewater and anaerobic digester effluent was investigated. Finally, we analyzed the economic effects of the proposed process compared to other ammonia recovery technologies. To our knowledge, this unique hybrid DD and solar energy-powered ED system for ammonia recovery have not previously been reported in the literature.

2. Materials and methods

2.1. Experiment setup and operations

The apparatus of the hybrid DD–ED process is shown in Fig. 1a. The flat-sheet membrane of an effective surface area of 26.6 cm^2 was assembled into the rectangular module, separating into two compartments in each process. For DD or ED process, a standard CEM, non-selective for monovalent cation (Neosepta CMX, ion exchange capacity of 1.5–1.8 meq g^{-1}) was used. For the ammonia recovery unit, a hydrophobic gas-permeable membrane (GPM) (Merck-Millipore GVHP, polyvinylidene fluoride, pore size of 0.22 μm) was used. For the module containing CEM, two commercial titanium mesh electrodes coated with ruthenium/iridium mixed metal oxide (Yunxuan Metal Materials Co., Ltd, China) were used, connected to a photovoltaic (PV) module consisting of solar panels (effective area of 1.5 m^2), voltage stabilizers, and lithium batteries (Shenzhen Nopro, China). An open circuit voltage of 15 V and a short circuit current of 5 A was provided after the battery was charged for 2 days (annual radiation ~1050 kWh m^{-2}) to drive the ED process (Fig. S1).

Two salts, NaCl and NH_4HCO_3 (Chongqing Chuandong, China, Reagent grade), were used. The effluent from an anaerobic digester fed by kitchen waste (68 mM NH_4^+, composition detailed in Table 1) was the real wastewater in this work. Since it was pre-filtered via microfiltration (of a nominal pore size of 0.45 μm), this wastewater

finally pumped into the membrane system exhibited a low suspended solid content of ca. 1 mg L^{-1}. Simple synthetic solution (NH_4HCO_3 of 10, 20, and 50 mM) or real wastewater were used as feed solution (i.e., anolyte in ED), respectively. The receiver (i.e., catholyte in ED) solution consisted of 90 mM NaCl (industrial salt, sodium chloride purity as 99.7%, referred to Table S1) and 10 mM NaOH, with a total Na^+ concentration of 100 mM. The initial presence of the low amount of alkali facilitates quick volatilization of the permeated NH_4^+, followed by efficient absorption in sulfuric acid (0.5 M H_2SO_4) [28]. Note: OH^- for ammonia stripping was provided by the cathodic reaction during the ED stage (equation (1)):

$$2H_2O + 2e^- \rightarrow H_2 + 2OH^- \tag{1}$$

The fresh feed solution was used in each experiment (cycle), whereas the receiver and the acid were unchanged for the three-cycle hybrid process, unlike in the standalone DD case, where both the feed and receiver were replaced in each cycle. All the solution was placed in a corresponding beaker (initial volume of 250 mL) atop of magnetic stirrer and circulated counter-currently across the membrane at a flow rate of 100 mL min^{-1} by a peristaltic pump (BT600 M, Chuang Rui, China) [29].

2.2. Principle of hybrid DD–ED process

Fig. 1b illustrates how the two consecutive stages of DD and ED were achieved (hybrid mode). In DD, NH_4^+ in the feed and Na^+ in the receiver undergo an exchange process across the CEM due to the concentration gradient, leading to an energy-free NH_4^+ removal at the cost of driving cation [27]. Then, in ED, both NH_4^+ and Na^+ in the feed migrate to the receiver across the CEM under the electrical potential to achieve further removal of NH_4^+ and recovery of the driving cation (Na^+). The GPM cell enables ammonia recovery due to the presence of alkali in the receiver chamber to transform ionic NH_4^+ into volatile NH_3 (Fig. 1c). Therefore, another merit of the hybrid DD–ED process beyond the transfer of NH_4^+ and Na^+ lies in the generation of OH^- at the cathode (by water reduction) during the intermittent ED process, which allows maintaining a high pH condition in the receiver chamber, facilitating the followed NH_3 absorption to generate high-purity NH_4^+-salt as a potential nitrogen fertilizer [30].

2.3. Determination of operating time in hybrid DD–ED process

ED stage was initiated once the DD process was nearly equilibrated or arrived at a low diffusion rate of target ions (NH_4^+), aiming to fully recover the driven cation (Na^+) and recover the remaining ammonia. A theoretical prediction of the DD performance was thus carried out by modeling the transfer of Na^+ and NH_4^+ under the charge balance, based on the study of Hirofumi Miyoshi et al. as detailed in equation (2) [29,31]. The model was derived according to the mass balance, and the good prediction of experimental data verifies the related hypothesis (Fig. S2).

$$\frac{dC_{A,F}}{dt} = -\frac{2D_A D_B Q S}{(D_A - D_B)L(V_F + V_R)} \\ \times \ln\left[\left\{\frac{C_{T_R}}{C_{T_F}}\right\} \times \left\{\frac{(D_A - D_B)C_{A_F} + D_B C_{T_F}}{(D_A - D_B)(C_{A_T} - C_{A_F}) + D_B C_{T_R}}\right\}\right] \tag{2}$$

where C (kmol m^{-3}), D (m^2 s^{-1}), and Q (kmol m^{-3}) are the concentration of ions in solution, diffusion coefficient, and exchange capacity of the ion-exchange membrane. Subscripts A and B represent A^+-ions and B^+-ions. L (m), S (m^2), and V (m^3) are the thickness of the membrane, the area of the membrane, and the volume of solution in the cell. The subscript T represents the total
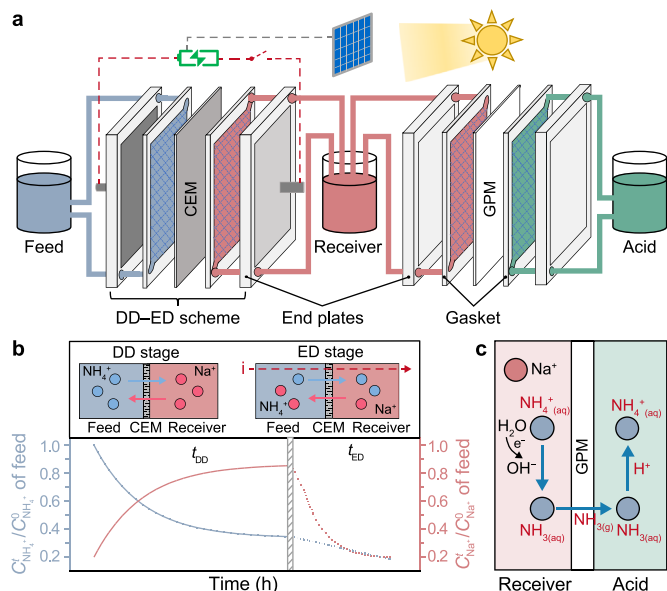
Fig. 1. **a**, The hybrid DD−ED scheme. The system contains a gas permeable membrane for ammonia recovery from NH_4^+-contained wastewater. **b**, The illustration of Na^+ and NH_4^+ concentration profile over time in the feed chamber as well as their transfer mechanism in DD and ED stages of the hybrid process. **c**, Ammonia transformation and recovery in the hybrid DD−ED system.

Fig. 2. Schematic representation of ammonia concentration profile (C_t/C_0) in the feed chamber (**a**) and current density profile (**b**) during the DD and ED stage in the proposed hybrid process. The extrapolated model was derived according to the study of Hirofumi Miyoshi et al., detailed in equation (2). The data shown in Fig. 2a was based on that under experiment conditions as: feed solution of $[NH_4HCO_3] = 50$ mM, receiver solution of $[Na^+] = 100$ mM, acid solution of $[H_2SO_4] = 0.5$ M. More data prediction refers to Fig. S2.

value, and subscripts F and R represent the Feed and Receiver chamber. The parameters required as input in equation (2) refer to Table S2. Fig. 2a describes the concentration profile of NH_4^+ in the feed was well predicted in the DD stage till T_1 when the process nearly reached the plateau according to the extrapolated model. Then, the duration of the ED stage (T_2-T_1) was calculated according to equation (3), given a default low current density (15 A m^{-2}), as shown in Fig. 2b. Assume that the experiment was carried out with L_{Na^+} equal to 1.2 considering that the excess current is used for Na^+ recovery [32].

$$L_{Na^+} = \frac{iAt}{C_{Na^+}VF} \quad (3)$$

where i is the current density (A m^{-2}), t is the time (s), A is the effective surface area of CEM (m^2), C_{Na^+} is the concentration (mol m^{-3}), V is the volume of the feed (m^{-3}), and F is the Faraday constant (96485 C mol^{-1}).

Considering concentration gradient may differentiate the kinetics of the DD stage or the time set of T_1 and T_2 from case to case [29], we determined the operating time in each experiment as t_{DD}/t_{ED} of 10/2, 11/3, 12/6, and 14/6 h for NH_4HCO_3 solution of 10, 20, 50 mM, and real wastewater (68 mM NH_4^+), respectively (Fig. S2).

2.4. Analytical approaches

Samples were collected at specific intervals (1 h) from the feed, receiver, and acid chamber. The concentration of ammonia (NH_3 and NH_4^+), driving cation (Na^+), and other impurities were determined by UV spectrophotometers (UV-2600, Shimadzu, Japan) and
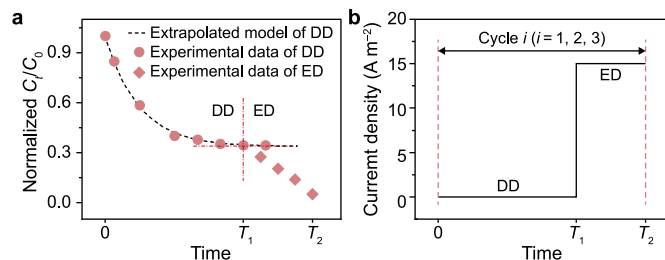
Ion Chromatography system (ICS-90, Dionex, USA), respectively. The solution pH value was measured by a pH meter (HI9811-5, HANNA, Italy). Each experiment was performed in triplicates, and the average data was used for the discussion.

The removal of NH_4^+ regarding the feed chamber and the recovery regarding the acid chamber were calculated respectively as:

$$\text{Removal of } NH_4^+ = 1 - \frac{C_f^t}{C_f^0} \quad (4)$$

$$\text{Recovery of } NH_4^+ = \frac{C_a^t}{C_f^0} \quad (5)$$

where C_f^0 and C_f^t are the ammonium concentrations in the feed at $t = 0$ and $t = t$, respectively. C_a^t represents the ammonium concentration in the acid at $t = t$, and the volume is constant during the reaction.

The ammonium flux across the CEM can be calculated as below:

$$J_{NH_4^+} = \frac{\left(C_{NH_4^+,f}^0 - C_{NH_4^+,f}^t\right) \times V_f}{A_m \times t} \quad (6)$$

where C represents the concentration of the specific ion at $t = 0$ and $t = t$, subscript f refers to the feed solution; V_f is the volume of the feed solution, and A_m is the CEM surface area.

Accumulated total energy consumption (kWh kg$_N^{-1}$) based on unit NH_4^+ recovered from the feed was calculated as follows:

$$E_a = \frac{\int IU \, dt}{1000 \times C_t \times V \times 14} \quad (7)$$

where U (V) is the cell voltage between the anode and cathode, I (A) is the applied current density in the DD stage, C_t (mol m^{-3}) is the difference between the NH_4^+ concentration at the initial time and at time t (h) and V is the volume of the feed (m^3).

The recovery of Na^+ regarding the receiver and the loss of Na^+ regarding the receiver was calculated as:

Table 1
Characteristics of the anaerobic digester effluent (Solution pH was ca. 8.8).

Parameter	Ammonia	COD	TP	TN	Na^+	K^+	Mg^{2+}	Ca^{2+}
Concentration (mg L^{-1})	950.0	106.2	1.9	980.0	288.8	345.6	23.1	34.9

$$\text{Loss of Na}^+ = \frac{C_{\text{Na}^+,\text{r}}^{t_0} - C_{\text{Na}^+,\text{r}}^{t_{\text{ED}}}}{C_{\text{Na}^+,\text{r}}^{t_0}} = \frac{C_{\text{Na}^+,\text{f}}^{t_0} - C_{\text{Na}^+,\text{f}}^{t_{\text{ED}}}}{C_{\text{Na}^+,\text{f}}^{t_0}} \qquad (8)$$

$$\text{Recovery of Na}^+ = \frac{C_{\text{Na}^+,\text{r}}^{t_{\text{ED}}} - C_{\text{Na}^+,\text{r}}^{t_{\text{DD}}}}{C_{\text{Na}^+,\text{r}}^{t_0} - C_{\text{Na}^+,\text{r}}^{t_{\text{DD}}}} = \frac{C_{\text{Na}^+,\text{f}}^{t_{\text{DD}}} - C_{\text{Na}^+,\text{f}}^{t_{\text{ED}}}}{C_{\text{Na}^+,\text{f}}^{t_{\text{DD}}} - C_{\text{Na}^+,\text{f}}^{t_0}} \qquad (9)$$

where $C_{\text{Na}^+,\text{r}}^{t_0}$, $C_{\text{Na}^+,\text{r}}^{t_{\text{DD}}}$, and $C_{\text{Na}^+,\text{r}}^{t_{\text{ED}}}$ are the sodium concentrations in the receiver at $t = t_0$, $t = t_1$ (end of DD stage), and $t = t_2$ (end of ED stage). Subscript r, f refers to receiver and feed.

The loss of OH⁻ in the receiver chamber due to the reaction with ammonium was calculated as:

$$\text{Loss of OH}^- = \frac{C_{\text{OH}^-,\text{r}}^{t_0} - C_{\text{OH}^-,\text{r}}^{t_{\text{ED}}}}{C_{\text{OH}^-,\text{r}}^{t_0}} \qquad (10)$$

where $C_{\text{OH}^-,\text{r}}^{t_0}$ and $C_{\text{OH}^-,\text{r}}^{t_{\text{ED}}}$ are the concentration of OH⁻ in the receiver stream at $t = t_0$ and $t = t_2$ (end of ED phase). The OH⁻ concentration is calculated according to $[\text{OH}^-] = 10^{-(14-\text{pH})}$

3. Results and discussion

3.1. Adaptability in varying NH₄⁺-N concentration

The process efficiency and feasibility were verified in experiments with low to moderate NH₄⁺ concentrations of synthetic wastewater (10, 20, 50 mM). Fig. 3a shows the variation of normalized concentration of NH₄⁺-N (C_t/C_0) in feed, receiver, and acid chamber, respectively, as a function of time under different initial NH₄⁺-N concentrations. In the DD stage, the ammonia removal in the feed gradually became slower in each case, and the ammonia recovery in the acid chamber was first rapid and then reached to plateau at the later stage of DD. During the ED stage, the slope of the ammonia concentration (C_t/C_0) curve for the

corresponding chamber became steeper. Clearly, adding an ED stage afterward increased ammonia removal and recovery. During the hybrid process, the accumulated ammonia in the receiver chamber continuously increased in the DD stage and then decreased quickly in the ED stage. The peak content of remaining ammonia in the receiver chamber increased with the initial feed concentration, in agreement with the importance of the concentration gradient of ionic species in DD. Fig. 3b shows the final removal of ammonia (equation (4)) in DD gradually decreased from 85.4% to 62.1% with the increase in ammonia concentration, while the total removal for the combined hybrid DD—ED process remained constant (~95%). Meanwhile, the recovery of ammonia (equation (5)) both in DD and hybrid DD—ED processes gradually decreased. Although a small amount of alkali was present in the receiver (OH⁻ of 10 mM) to initiate the volatilization and stripping of ammonia, the alkali was insufficient for complete ammonia recovery in these three conditions (10, 20, and 50 mM). Then, the herein DD stage can be regarded as a Na⁺ (100 mM) driven ion-exchange process toward NH₄⁺. Thus, the final equilibrated removal in this work was considered close to that in normal DD operation (without alkali supply to strip ammonia), which explains the decreasing recovery trend with increasing ammonia concentration. Then, the decreased recovery in the DD agreed with the clearer lack of alkali in the receiver chamber concerning the removed ammonia. After the ED stage, a higher removal and recovery in line with the stimulated concentration profile in Fig. 3a confirmed the positive impact of the ED process in further ammonia removal (Fig. 1b) on the one hand and favored the volatilization of ammonia (ammonia recovery) and alkali production. Fig. 3c showed the NH₄⁺ flux across CEM (equation (6)) in both processes increased, and the difference became more obvious with the increase in ammonia concentration. Interestingly, the energy demand for ammonia recovery per unit nitrogen of the hybrid process (equation (7)) gradually decreased, mainly due to the increased amount of ammonia recovered concerning the energy supplied.

Meanwhile, our result also suggests that the operating methodology proposed in Section 2.3 was a precise prediction and control of the DD stage in hybrid processes at different ammonia concentrations. Since increasing the ammonia concentration exhibited a positive effect on NH₄⁺ flux and energy efficacy in the hybrid process, the following experiments were thus carried out at a concentration of 50 mM NH₄⁺-N, to verify the feasibility and stability of the hybrid process operated in multiple hybrid DD—ED cycles.

3.2. Merits of hybrid DD—ED process in multi-cycle mode

3.2.1. Enhanced recovery of ammonia

The continuous reduction and increase in ammonia concentration in the feed and acid, respectively, during the three-cycle operation of the hybrid process, was shown in Fig. 4a. The final ammonia concentration in the acid chamber was as high as 2372 mg L⁻¹ with a recovery of 85.6%. As shown in Fig. 4b, the removal of the hybrid process was high at 95.5% compared to the ~64.8% during the DD process, also superior to those alternative recovery processes (38—88%, Table S4) at comparable NH₄⁺ concentration. In addition, the recovery of ammonia gradually increased from 73.2% to 94.4%, ~2 to 3-fold that in the DD process (~30.6%). This could be ascribed to the continuous transfer of ammonia from the previous cycle assisted by the OH⁻ generated at the cathode during the ED stage [18]. Thus, the averaged NH₄⁺-N flux of the hybrid DD—ED process (99.1 g_N d⁻¹ m⁻²) increased by 60.2% compared with the DD process (61.9 g_N d⁻¹ m⁻²) (Fig. 4f).
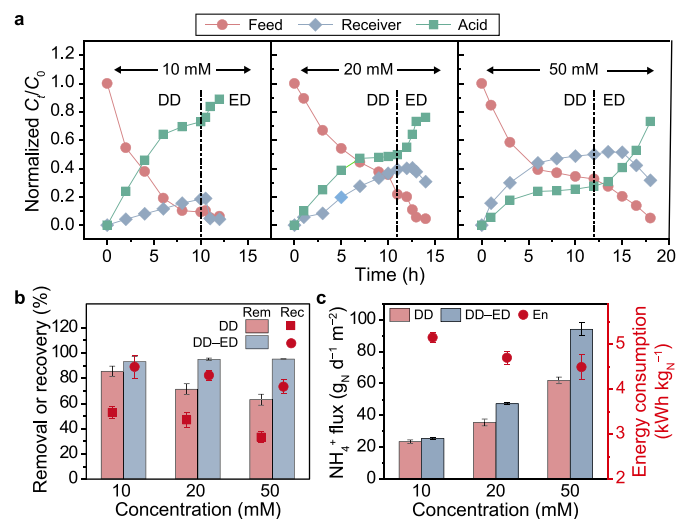
Fig. 3. a, Normalized NH₄⁺-N concentration (C_t/C_0) versus time in the hybrid DD—ED process. **b—c**, The removal and recovery of NH₄⁺-N (**b**) and the corresponding flux across CEM and energy consumption (**c**) at NH₄⁺-N concentration of 10, 20, and 50 mM, respectively. To highlight the adaptability of the process in varying concentrations, normalized data were used in Fig. 3a. Rem and Rec denote removal and recovery in Fig. 3b, and En denotes energy consumption in Fig. 3c, respectively. The initial condition was: Na⁺ concentration in the receiver solution = 100 mM (90 mM NaCl + 10 mM NaOH), H₂SO₄ concentration in the acid solution = 0.5 M.

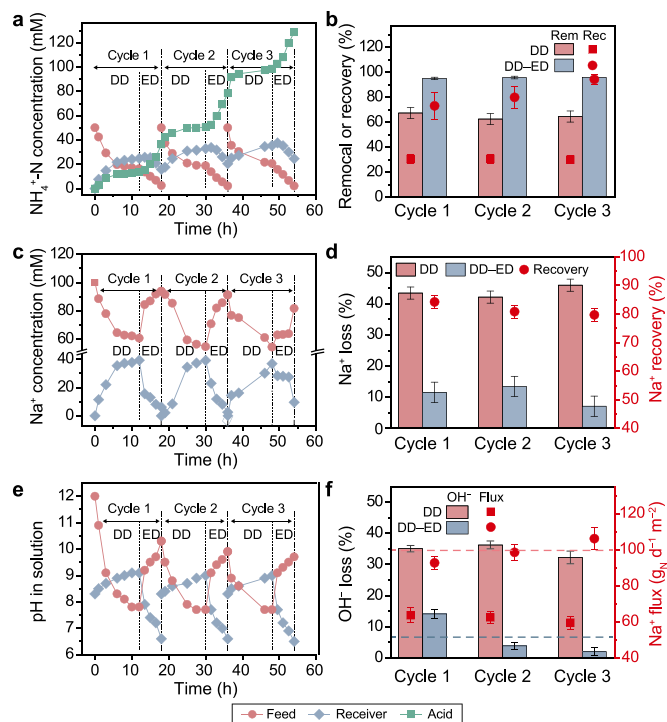**Fig. 4.** Performance of hybrid DD−ED process in the three-cycle operation: NH_4^+-N concentration (**a**), Na^+ concentration (**c**), and solution pH (**e**) versus time, as well as NH_4^+-N removal and recovery (**b**), Na^+ loss and recovery (**d**), OH^- loss and NH_4^+ flux across CEM (**f**) in respect with that in DD standalone. Rem and Rec denote removal and recovery, respectively, in Fig. 4b. Initial condition was: NH_4HCO_3 concentration in the feed solution = 50 mM, Na^+ concentration in the receiver solution = 100 mM (90 mM NaCl + 10 mM NaOH), H_2SO_4 concentration in the acid solution = 0.5 M.

3.2.2. Reduced loss of driving cation

As shown in Fig. 4c, the Na^+ concentration in the receiver first decreased in DD and then increased in ED, and the Na^+ concentration in the feed changed correspondingly. The herein transfer of Na^+ was mainly driven by first the concentration difference (DD) and then the potential difference (ED) under constant current mode. Ammonia recovery was at the cost of losing the driving cation (i.e., Na^+) to the feed in the DD process, potentially impacting a subsequent wastewater treatment process by inhibiting microbial activity [29,33,34]. The recovered driving ion after the ED stage facilitated the reduction of ammonium in the next DD stage. A small loss of driving ions in the receiver solution after each cycle was found, as indicated by gradually reduced Na^+ concentration compared to the initial value. While such an inevitable loss did affect the concentration gradient of Na^+ across CEM, the performance of the next DD stage was predictable, with a maximum deviation <6% according to our proposed model (Figs. S3a−c). Our results implied the need for a delicately operating strategy of the hybrid process in the future long-term run. The Na^+ loss for the three cycles in DD and the overall hybrid DD−ED process was stable and averaged 43.8% and 10.7%, respectively. In other words, the Na^+ loss of the hybrid process was reduced by 75.6%, with 87.1% of the initial Na^+ recovered back to the receiver (Fig. 4d).

3.2.3. Alleviated consumption of OH^-

The pH variation in the feed and receiver chamber with time in the hybrid DD−ED process is shown in Fig. 4e. The pH value in the receiver chamber dropped from 12 to 7.7 (slightly alkaline) in the DD stage of the first cycle. Such a phenomenon can be ascribed to the OH^- consumption due to the reaction with NH_4^+ diffused from

the feed and the leakage of OH^- across the CEM, which also explained the slight increase of the pH value in the feed. Interestingly, as shown in Fig. 4e, when the pH in the feed was higher than that in the receiver, a slight upward trend for the feed pH was still found, which appears to disagree with OH^- leakage. This can be mainly attributed to the change in NH_4^+/HCO_3^- concentration (i.e., buffer species) in the feed chamber and the occurrence of hydrolysis of species, which was out of the main scope of our work [35]. In the ED stage of each cycle, the pH value in the receiver chamber increased to higher than 9.3, which led to NH_3 dominance for the NH_4^+-NH_3 buffer pair and, consequently, a successful ammonia recovery (Fig. 4a). Compared with the DD process, the OH^- loss in the DD−ED hybrid process was reduced by 78.0% (Fig. 4f). Moreover, a gradually decreased loss of OH^- during the three-cycle hybrid DD−ED process was found, which was mainly ascribed to the decrease of the initial pH caused by alkali leakage, according to equation (10).

3.3. Ammonia recovery from anaerobic digester effluent fed with kitchen waste

The performance of the hybrid DD−ED hybrid process was investigated by treating anaerobic digester effluent fed with kitchen waste (NH_4^+ concentration of 68 mM). A stable NH_4^+ removal of 82.0% and ammonia recovery of 71.2% for the hybrid DD−ED process dealing with the real wastewater was shown in Fig. 5a. With the final ammonium concentration reaching ~2600 mg L^{-1}, and no other competing cations (i.e., K^+, Mg^{2+}, and Ca^{2+}) present in the real wastewater detected in the acid chamber, a high-purity ammonium sulfate solution was produced. However, Fig. 5a also shows the migration of other co-existing cations to the receiver, with a maximum concentration of 9.1 and 1.3 mM for K^+ and divalent ions (i.e., Ca^{2+}, Mg^{2+}) after the three-cycle operation. In terms of overall transfer quantity for these ionic species, the value for NH_4^+ (14.5 mmol) outcompeted other co-cation ions (2.3 and 0.33 mmol for the mono- and di-valent species, respectively). The SEM data for membranes coupons after the three-cycle
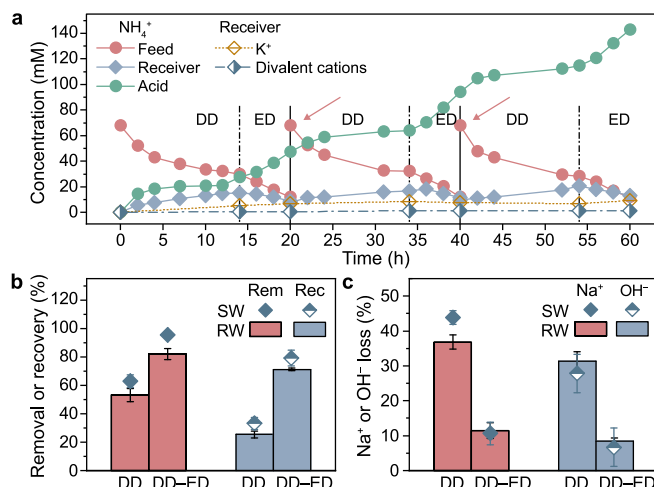

Fig. 5. Performance of hybrid DD−ED process in the three-cycle operation: NH_4^+-N concentration (**a**), the corresponding removal and recovery (**b**), and the Na^+ and OH^- loss (**c**). Fresh feed was used in each cycle, as indicated by the pink arrow in Fig. 5a. SW and RW denote synthetic wastewater and real wastewater, respectively, in Fig. 5b and **c**. Rem and Rec denote removal and recovery, respectively, in Fig. 5b. Initial condition was: in the feed solution, NH_4HCO_3 concentration = 50 Mm for SW or anaerobic digester effluent concentration = 68 mM for RW, Na^+ concentration in the receiver solution = 100 mM (90 mM NaCl + 10 mM NaOH), H_2SO_4 concentration in the acid solution = 0.5 M.

operation revealed no difference in surface and cross-section morphology of the membrane compared to the pristine one for GPM and CEM, respectively (Fig. S4). The anti-fouling potential of the hybrid process would be worthwhile for future studies. Such a result could be ascribed to not only the privilege of concentration, as in Table 1, but also of diffusivity for NH_4^+, especially compared to the divalent cations [29,36]. As shown in Fig. 5b, the process performance of treating the real wastewater was slightly inferior to that of a simple synthetic solution by ~10% for both the removal and recovery. Such a result suggests the complex nature of real wastewater exhibited a small detrimental effect on the recovery process. Moreover, the slightly higher loss rates of Na^+ and OH^- in the hybrid process with the real wastewater in Fig. 5c were mainly due to the competition of impurity ions (i.e., K^+, Mg^{2+}, Ca^{2+}) with Na^+ to be recovered in the ED process, and potential consumption of a part of OH^- by the migrated impurity ions (i.e., Mg^{2+}, Ca^{2+} from the feed to receiver chamber (Fig. 5a and Table S3). Fortunately, a previous study showed that given monovalent selective cation exchange membranes (e.g., Selemion CSO), the aforementioned adverse impacts of divalent ion migration in the ammonia recovery process could be minimized [29]. In addition, the pH value of the receiver chamber exhibited a similar repeating pattern (increasing from 7.9 to around 11.6) in each cycle, in line with the data for synthetic solution (Fig. 4e), favoring the continuous recovery of ammonia considering the pKa value approximating to 9.3 (Fig. S5a). The ammonia flux of the hybrid DD—ED process with real wastewater reached 98.2 g_N d^{-1} m^{-2} with the input energy of 3.82 kWh kg_N^{-1} utilizing solar energy. Compared with the synthetic solution, the energy consumption of the hybrid process for real wastewater was reduced by 19.1% (Fig. S5b). This may be due to the higher NH_4^+ concentration and lower internal resistance caused by the higher conductivity in real wastewater [2]. Interestingly, the performance of the DD stage in the hybrid process treating real stream could be predicted by the model (equation (2)) with the parameters input (Figs. S3d—f). When the predicted removal efficiency of the DD process is lower than the expected value, in other words, the multi-cycle of the hybrid DD—ED process should be ended, and the driving ions should be supplemented into the receiver chamber to maximize the effect of energy-free NH_4^+ removal via the DD process. In summary, the hybrid DD—ED process can stably achieve efficient ammonia recovery from the effluent of an anaerobic digester fed with kitchen waste.

3.4. Comparison with other ammonia recovery processes

Fig. 6 compares the energetics of reported ammonia recovery processes. As most were electrical-driven processes (pink colored), their performance and energy efficacy are highly associated with the applied current density [32]. The required electrical energy ranges from 5 to 25 kWh kg_N^{-1}, considering the assistance of cultivated biomass, which effectively converts the chemical energy contained in wastewater into electricity, generally referred to as the bio-electrochemical (BES) process [37]. However, adequate conditions for robust bioactivity are not easily maintained in long-term operations. In contrast, the intermittent assistance of DD or ED is prospective in lowering the specific energy input (green colored). At 3.82 kWh kg_N^{-1} (solar energy input, according to equation (7)), the herein hybrid DD—ED process achieved NH_4^+-N fluxes as high as 98.2 gN d^{-1} m^{-2} comparable to ES fluxes at higher current densities dealing with moderate-strength wastewater (Table S4). Despite the energy consumption of the hybrid process seeming higher compared with that in the standalone DD case (2.06 kWh kg_N^{-1}), the performance of the hybrid process is, in fact, much improved (Fig. 6), with further application potential under off-grid mode (e.g., solar energy input). Our NH_4^+ removal data was also superior to
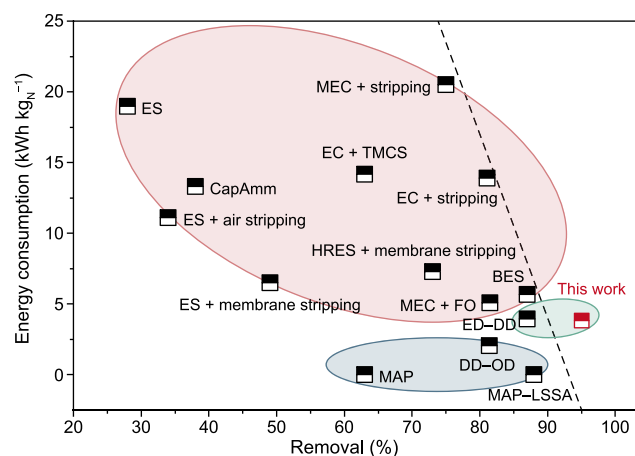

Fig. 6. Energy consumed per unit of N versus the removal from the feed solution under moderate to high initial NH_4^+ concentration (>50 mM or 700 mg L^{-1}). The pink area represents the electrochemical processes, the blue area represents the non-electrochemical processes, and the green area represents the process with partial electricity assistance. MEC: Microbial Electrolysis Cell. CapAmm: Capacitive membrane stripping for Ammonia recovery. TMCS: TransMembrane ChemiSorption. BES: Bio-electrochemical Process. MEC—FO: Microbial Electrolysis Cell and Forward Osmosis hybrid process. ES: Non-biological electrochemical process. HRES: H_2 recycling electrochemical process. EC: Electrochemical cell. MAP: Struvite precipitation. MAP—LASS: Struvite precipitation-leachate of sewage sludge ash. DD—OD: Donnan Dialysis—Osmotic Distillation. ED—DD: Electrochemical system—Donnan Dialysis. The energy-efficiency profile of the DD—ED hybrid process in moderate NH_4^+-N strength is denoted as "this study". The herein energy consumption of the DD—ED system originated from solar energy from photovoltaic panels.

conventional processes, including struvite precipitation (blue colored), which often suffers a series of problems like high chemical usage and secondary pollution [8,9]. Therefore, the prospective efficiency of the hybrid process was again highlighted, as illustrated in Fig. 6 and Table S4.

The economic evaluation of NH_4^+ recovery via the hybrid DD—ED process was calculated based on treating effluent from an anaerobic digester for kitchen waste with 1224 mg L^{-1} NH_4^+ (68 mM) and 5 m^3 d^{-1} wastewater (Fig. S6). Inputs, assumptions, and the calculation process are detailed in Tables S5—S6 [8,38—42]. Considering the value of recycled N, the net cost of the hybrid DD—ED process was $1358 year^{-1} at a recovery cost of $3.8 kg_N^{-1}, much lower than the gas-permeable membrane system without aeration for a comparable waste stream ($10.1 kg_N^{-1}) [38]. This result suggests that the hybrid DD—ED process has great economic potential for ammonia recovery from N-containing wastewater. It is noteworthy that potential environmental and ecological benefits are not included in this analysis, and we argue that reduced greenhouse gas (direct and/or indirect N_2O) emissions and the risk of eutrophication of water bodies would further increase the benefit of this ammonia recovery process.

4. Conclusion

Our study proposed efficient and sustainable ammonia removal and recovery from wastewater by a hybrid Donnan dialysis—electrodialysis (DD—ED) process, which exploits industrial salt as a driving substance in DD and solar energy as the driving power in ED. A hypothesis was developed that both the transfer of NH_4^+ and driving cation (Na^+) can be manipulated to efficiently recover ammonia in such a system, with appropriate pH conditions due to intrinsic Faradaic reaction favoring the conversion of NH_4^+ to NH_3. Guiding by the modeled mass transfer, the hybrid DD—ED process achieved ammonia removal efficiency >95% and Na^+

recovery efficiency >87% and reduced the OH^- loss rate by up to 78% compared to DD standalone case. Ammonia fluxes of 98.2 g_N m^{-2} d^{-1} were observed at 3.82 kWh kg_N^{-1} in dealing with the effluent of an anaerobic digester fed with kitchen waste. Future work may further investigate the long-term performance of the up-scaled module under automatic control for nutrient recovery from wastewater, especially in remote rural areas.

CRediT authorship contribution statement

Zhinan Dai: Conceptualization, Investigation, Methodology, Formal analysis, Writing - original draft. **Cong Chen**: Formal analysis, Validation, Visualization. **Yifan Li**: Formal analysis, Visualization. **Haoquan Zhang**: Formal analysis, Visualization. **Mariana Rodrigues**: Writing - review & editing. **Philipp Kuntke**: Writing - review & editing. **Jingmei Yao**: Writing - review & editing. **Le Han**: Supervision, Writing - review &editing, Funding acquisition.

Declaration of competing interest

The authors declare that they have no potential conflicts of interest with respect to the research, authorship or publication of this article.

Acknowledgement

Appendix A. Supplementary data

Supplementary data to this article can be found online at https://doi.org/10.1016/j.ese.2023.100255.

References

[1] H. Cruz, Y.Y. Law, J.S. Gues, K. Rabaey, D. Batstone, B. Laycock, W. Verstraete, I. Pikaar, Mainstream ammonium recovery to advance sustainable urban wastewater management, Environ. Sci. Technol. 53 (2019) 11066–11079.

[2] C. Zhang, J. Ma, J. Song, C. He, T.D. Waite, Continuous ammonia recovery from wastewaters using an integrated capacitive flow electrode membrane stripping system, Environ. Sci. Technol. 52 (2018) 14275–14285.

[3] Y. Li, R. Wang, S. Shi, H. Cao, N.Y. Yip, S. Lin, Bipolar membrane electrodialysis for ammonia recovery from synthetic urine: experiments, modeling, and performance analysis, Environ. Sci. Technol. 55 (2021) 14886–14896.

[4] H. Dong, C.M. Laguna, M.J. Liu, J. Guo, W.A. Tarpeh, Electrified ion exchange enabled by water dissociation in bipolar membranes for nitrogen recovery from source-separated urine, Environ. Sci. Technol. 56 (2022) 16134–16143.

[5] F. Ferrari, M. Pijuan, S. Molenaar, N. Duinslaeger, T. Sleutels, P. Kuntke, J. Radjenovic, Ammonia recovery from anaerobic digester centrate using onsite pilot scale bipolar membrane electrodialysis coupled to membrane stripping, Water Res. 218 (2022), 118504.

[6] S. Wang, Y. Peng, Natural zeolites as effective adsorbents in water and wastewater treatment, Chem. Eng. J. 156 (2010) 11–24.

[7] J. Huang, N.R. Kankanamge, C. Chow, D.T. Welsh, T. Li, P.R. Teasdale, Removing ammonium from water and wastewater using cost-effective adsorbents: a review, J. Environ. Sci. 63 (2018) 174–197.

[8] Y. Ye, H.H. Ngo, W. Guo, Y. Liu, S.W. Chang, D.D. Nguyen, H. Liang, J. Wang, A critical review on ammonium recovery from wastewater for sustainable wastewater management, Bioresour. Technol. 268 (2018) 749–758.

[9] M.S. Romero-Gueiza, S. Tait, S. Astals, R. del Valle-Zermeno, M. Martinez, J. Mata-Alvarez, J.M. Chimenos, Reagent use efficiency with removal of nitrogen from pig slurry via struvite: a study on magnesium oxide and related by-products, Water Res. 84 (2015) 286–294.

[10] S. Antonini, S. Paris, T. Eichert, J. Clemens, Nitrogen and phosphorus recovery from human urine by struvite precipitation and air stripping in vietnam, Clean: Soil, Air, Water 39 (2011) 1099–1104.

[11] A.J. Ward, K. Arola, E.T. Brewster, C.M. Mehta, D.J. Batstone, Nutrient recovery from wastewater through pilot scale electrodialysis, Water Res. 135 (2018) 57–65.

[12] F. Waeeger-Baumann, W. Fuchs, The application of membrane contactors for the removal of ammonium from anaerobic digester effluent, Separ. Sci. Technol. 47 (2012) 1436–1442.

[13] T. Yan, Y. Ye, H. Ma, Y. Zhang, W. Guo, B. Du, Q. Wei, D. Wei, N. Huu Hao, A critical review on membrane hybrid system for nutrient recovery from wastewater, Chem. Eng. J. 348 (2018) 143–156.

[14] W. Lee, S. An, Y. Choi, Ammonia harvesting via membrane gas extraction at moderately alkaline pH: a step toward net-profitable nitrogen recovery from domestic wastewater, Chem. Eng. J. 405 (2021).

[15] S. Daguerre-Martini, M.B. Vanotti, M. Rodriguez-Pastor, A. Rosal, R. Moral, Nitrogen recovery from wastewater using gas-permeable membranes: impact of inorganic carbon content and natural organic matter, Water Res. 137 (2018) 201–210.

[16] C. Chen, Z. Dai, Y. Li, Q. Zeng, Y. Yu, X. Wang, C. Zhang, L. Han, Fouling-free membrane stripping for ammonia recovery from real biogas slurry, Water Res. 229 (2023), 119453-119453.

[17] M.J. Liu, B.S. Neo, W.A. Tarpeh, Building an Operational Framework for Selective Nitrogen Recovery via Electrochemical Stripping, 169, Water Research, 2020.

[18] G. Lee, D. Kim, J.I. Han, Gas-diffusion-electrode based direct electro-stripping system for gaseous ammonia recovery from livestock wastewater, Water Res. 196 (2021), 117012.

[19] M. Rodrigues, A. Paradkar, T. Sleutels, A.T. Heijne, C.J.N. Buisman, H.V.M. Hamelers, P. Kuntke, Donnan Dialysis for scaling mitigation during electrochemical ammonium recovery from complex wastewater, Water Res. 201 (2021), 117260.

[20] W.A. Tarpeh, J.M. Barazesh, T.Y. Cath, K.L. Nelson, Electrochemical stripping to recover nitrogen from source-separated urine, Environ. Sci. Technol. 52 (2018) 1453–1460.

[21] A. Iddya, D. Hou, C.M. Khor, Z. Ren, J. Tester, R. Posmanik, A. Gross, D. Jassby, Efficient ammonia recovery from wastewater using electrically conducting gas stripping membranes, Environmental Science-Nano 7 (2020) 1759–1771.

[22] P. Kuntke, M.R. Arredondo, L. Widyakristi, A. ter Heijne, T.H.J.A. Sleutels, H.V.M. Hamelers, C.J.N. Buisman, Hydrogen gas recycling for energy efficient ammonia recovery in electrochemical systems, Environ. Sci. Technol. 51 (2017) 3110–3116.

[23] M. Rodrigues, T. Sleutels, P. Kuntke, D. Hoekstra, A. ter Heijne, C.J.N. Buisman, H.V.M. Hamelers, Exploiting Donnan Dialysis to enhance ammonia recovery in an electrochemical system, Chem. Eng. J. 395 (2020).

[24] J. Uche, F. Cirez, A.A. Bayod, A. Martinez, On-grid and off-grid batch-ED (electrodialysis) process: simulation and experimental tests, Energy 57 (2013) 44–54.

[25] N. Mir, Y. Bicer, Thermodynamic modeling of a combined photo-electrodialysis-chloralkali system for sustainable desalination, Desalination (2021) 499.

[26] P. Malek, J.M. Ortiz, H.M.A. Schulte-Herbrueggen, Decentralized desalination of brackish water using an electrodialysis system directly powered by wind energy, Desalination 377 (2016) 54–64.

[27] S. Sarkar, A.K. Sengupta, P. Prakash, The donnan membrane principle: opportunities for sustainable engineered processes and materials, Environ. Sci. Technol. 44 (2010) 1161–1166.

[28] C. Chen, M. Han, J. Yao, Y. Zhi, Y. Liu, C. Zhang, L. Han, Donnan dialysis-osmotic distillation (DD-OD) hybrid process for selective ammonium recovery driven by waste alkali, Environ. Sci. Technol. 55 (2021) 7015–7024.

[29] C. Chen, T. Dong, M. Han, J. Yao, L. Han, Ammonium recovery from wastewater by Donnan Dialysis: a feasibility study, J. Clean. Prod. (2020) 265.

[30] M. Rodrigues, R.J. Lund, A. ter Heijne, T. Sleutels, C.J.N. Buisman, P. Kuntke, Application of ammonium fertilizers recovered by an electrochemical system, resources, Conserv. Recycl. (2022) 181.

[31] H. Miyoshi, Diffusion coefficients of ions through ion exchange membrane in Donnan dialysis using ions of different valence, J. Membr. Sci. 141 (1998) 101–110.

[32] M. Rodriguez Arredondo, P. Kuntke, A. Ter Heijne, H.V.M. Hamelers, C.J.N. Buisman, Load ratio determines the ammonia recovery and energy input of an electrochemical system, Water Res. 111 (2017) 330–337.

[33] J. Li, L. Bai, Z. Qiang, H. Dong, D. Wang, Nitrogen removal through "Candidatus Brocadia sinica" treating high-salinity and low-temperature wastewater with glycine addition: enhanced performance and kinetics, Bioresour. Technol. 270 (2018) 755–761.

[34] Y. Liu, Y.-Y. Deng, Q. Zhang, H. Liu, Overview of Recent Developments of Resource Recovery from Wastewater via Electrochemistry-Based Technologies, Science of the Total Environment, 2021, p. 757.

[35] Y. Fu, Y.-z. Wang, M.-m. Su, Hydrolysis performance of poly-Al-Fe containing zinc (PAZF) coagulant and its removal of color and organic matters, J. Water Proc. Eng. 4 (2014) 58–66.

[36] L. Han, S. Galier, H. Roux-de Balmann, Ion hydration number and electro-osmosis during electrodialysis of mixed salt solution, Desalination 373 (2015) 38–46.

[37] P. Kuntke, T. Sleutels, M.R. Arredondo, S. Georg, S.G. Barbosa, A. ter Heijne,

H.V.M. Hamelers, C.J.N. Buisman, (Bio)electrochemical ammonia recovery: progress and perspectives, Appl. Microbiol. Biotechnol. 102 (2018) 3865−3878.

[38] P.J. Dube, M.B. Vanotti, A.A. Szogi, M.C. Garcia-Gonzalez, Enhancing recovery of ammonia from swine manure anaerobic digester effluent using gas-permeable membrane technology, Waste Manag. 49 (2016) 372−377.

[39] D.G. Randall, J. Nathoo, Resource recovery by freezing: a thermodynamic comparison between a reverse osmosis brine, seawater and stored urine, J. Water Proc. Eng. 26 (2018) 242−249.

[40] X. Li, W. Zhu, Y. Wu, C. Wang, J. Zheng, K. Xu, J. Li, Recovery of potassium from landfill leachate concentrates using a combination of cation-exchange membrane electrolysis and magnesium potassium phosphate crystallization, Separ. Purif. Technol. 144 (2015) 1−7.

[41] A. Beckinghausen, M. Odlare, E. Thorin, S. Schwede, From removal to recovery: an evaluation of nitrogen recovery techniques from wastewater, Appl. Energy (2020) 263.

[42] S. Alobaidani, E. Curcio, F. Macedonio, G. Diprofio, H. Alhinai, E. Drioli, Potential of membrane distillation in seawater desalination: thermal efficiency, sensitivity study and cost estimation, J. Membr. Sci. 323 (2008) 85−98.